Rare Metal Materials and Engineering
Volume 51, Issue 7, July 2022
Available online at www.rmme.ac.cn

Science Press

Cite this article as: Chen Haoran, Yang Liangwei, Zhang Baopeng, et al. Effects of HfC-TaC Modification on Static Oxidation Behavior of C/SiC-ZrC Composites[J]. Rare Metal Materials and Engineering, 2022, 51(07): 2349-2355.

ARTICLE

Effects of HfC-TaC Modification on Static Oxidation Behavior of C/SiC-ZrC Composites

Chen Haoran, Yang Liangwei, Zhang Baopeng, Liu Wei, Song Huanjun

Research Institute of Aerospace Special Materials and Processing Technology, Beijing 100074, China

Abstract: HfC-TaC was employed to modify the C/SiC-ZrC composites and to improve their oxidation resistance. The composites were fabricated by the combined process of precursor infiltration and pyrolysis method and chemical vapor deposition method, and the oxidation resistance was evaluated by static oxidation tests (1600 °C/5 h and 1600 °C/20 h). According to the test results of flexural strength and mass loss, it is found that HfC-TaC can effectively improve the anti-oxidation behavior of C/SiC-ZrC composites without obviously decreasing their mechanical properties. By virtue of X-ray diffraction, scanning electron microscopy, and energy dispersive spectrometry, the crystal structure and microstructure of composites were analyzed. Results show that the superior anti-oxidation behavior of C/SiC-ZrC composites after HfC-TaC modification can be ascribed to the uniform element distribution and well-integrated components in the matrix.

Key words: HfC-TaC; C/SiC-ZrC; ceramic matrix composites; static oxidation; precursor infiltration and pyrolysis

Over the past decades, great demands of structural materials of low density as well as excellent mechanical and oxidation resistance properties in extreme environments are excited for the components of aerospace vehicles, such as turbine engines, leading edges, and nose caps[1]. The conventional thermal-structural materials, such as alloys, C/C composites, and ultra-high temperature ceramics (UHTCs), cannot simultaneously meet requirements of low density, good mechanical properties, as well as excellent oxidation resistance at high temperature. However, continuous carbon-fiber-reinforced ceramic matrix composites (CMCs) with lower density overcome the inherent brittleness of UHTCs and exhibit better oxidation resistance than C/C composites do[2-5]. Therefore, CMCs become one of the most promising materials in aerospace and aviation fields[6-8].

The outstanding oxidation resistance of CMCs is derived from their unique structures, consisting of continuous carbon fiber, interface phase, ceramic matrix, and coating. Among these four components of CMCs, the ceramic matrix plays an important role in the overall oxidation resistance and mechanical property. In order to serve under severe conditions, CMCs need further modification of matrix to enhance the anti-oxidation property at high temperature. C/SiC-ZrC composite has been identified as one of the most promising CMCs[9]. The combination of ZrC and SiC results in the formation of SiO_2 and $ZrSiO_4$ during the oxidation, acting as the effective barrier against the oxidation[10-12]. Zhou et al[13] studied the relationship between mass loss and oxidation time of C-SiC-ZrC composites from 1000 °C to 1200 °C, and found that a sharp mass loss (nearly 9%) appears after oxidation at 1000 °C for 60 min. This result indicates that the oxidation resistance of SiC-ZrC requires further enhancement.

In order to further improve the long-time oxidation resistance of composites, HfC and TaC are introduced into the ceramic matrix[14,15]. As the melting points of refractory metal carbides are close to 4000 °C[16], HfC and TaC both exhibit unique advantages in terms of oxidation resistance. Shimada et al[17] reported that the three-layer structures appear at the cross section of composites: the residual HfC layer, dense carbon-containing HfO_2 interface layer, and porous HfO_2 layer. Among these three layers, the carbon-containing HfO_2 interface layer possesses a stronger oxygen diffusion barrier, effectively improving the oxidation resistance of composites. Chen et al[18] prepared the C/C-TaC composites via chemical vapor infiltration method and studied their oxidation behavior

---

Received date: July 09, 2021

Corresponding author: Chen Haoran, Ph. D., Engineer, Research Institute of Aerospace Special Materials and Processing Technology, Beijing 100074, P. R. China, E-mail: chenhaoran@pku.edu.cn

at elevated temperatures. It is found that the mass increases at 900~1300 °C and decreases at 1400 °C; while the acute mass loss occurs when the temperature further increases to 1500 °C.

In this research, the C/SiC-ZrC and C/SiC-ZrC-HfC-TaC composites were fabricated via combined process of precursor infiltration and pyrolysis (PIP) method and chemical vapor deposition (CVD) method. The oxidation resistance of composites was evaluated through mass loss rate and flexural strength retention after static oxidation tests at 1600 °C. Influences of HfC-TaC modification on anti-oxidation properties of C/SiC-ZrC composites were also discussed according to the microstructures, morphologies, and element distribution.

1 Experiment

The needle-punched (T700 12k) carbon fiber preforms (Yixing Tianniao High Technology Co., Ltd, Jiangsu, China) with the density of 0.4 g/cm^3 were used as the reinforcements of composites. Zirconium-silicon (ZS) and tantalum-hafnium-carbon (THC) precursors (Institute of Chemistry, Chinese Academy of Sciences) were used to prepare SiC-ZrC matrix and HfC-TaC matrix, respectively. Propane, hydrogen, argon, and methyltrichlorosilane (MTS, CH_3SiCl_3) were all at analytical grade.

The needle-punched preforms were used as the skeleton, and the pyrolytic carbon (PyC) interface layer was prepared with propane as precursor until the density reached about 1.0 g/cm^3. Subsequently, the preforms were infiltrated with the solution of ZS precursor and then pyrolyzed under inert atmosphere. PIP process was repeated until the ratio of mass gain was less than 1%. Finally, the SiC coating was prepared with MTS-H_2-Ar as the precursor system.

The preparation of C/SiC-ZrC-HfC-TaC composites was also conducted through the similar procedures. After the deposition of PyC interface phase, the SiC-ZrC matrix was obtained by repeated PIP process using ZS precursor until the the bulk density reached ~2.1 g/cm^3. Then HfC-TaC modification was realized using THC precursor via PIP process. The densification process was finished when the ratio of mass gain was lower than 1%. At last, the SiC coating was deposited to protect the interior ceramic matrix and carbon fiber from oxidation at high temperature.

Three-point bending test was conducted by the CSS44050 electronic universal testing machine. Bending tests were conducted according to Q/SB 513-2013 standard, and the specimen size was 60 mm×9 mm×4 mm (Fig. 1). During the test, the crosshead speed was 0.5 mm/min with the support span of 40 mm. The flexural strength σ was calculated by Eq.(1), as follows:

$$\sigma = \frac{3PL}{2bh^2} \tag{1}$$

where L, h, and b denote the span of bending test, the specimen thickness, and the specimen width, respectively; P is the maximum applied load during testing.

The oxidation resistance of composites was evaluated by the static oxidation experiments in the muffle furnace. The temperature was firstly increased to 1600 °C at the heating rate of 5 °C/min. Then the specimens were placed in the furnace center for 5 or 20 h. Finally, the specimens were directly taken out at 1600 °C and cooled down at room temperature. The mass loss rates were obtained and calculated according to the specimen mass before and after the oxidation experiments. The mass loss rate (R_m) can be calculated by Eq.(2), as follows:

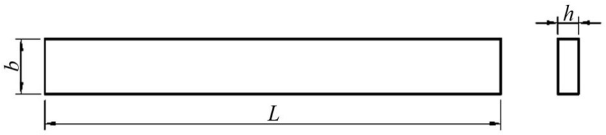

Fig.1 Schematic diagram of shape and size of bending specimen (L=60 mm; b=9 mm; h=4 mm)

$$R_m = \frac{m_0 - m_t}{t} \tag{2}$$

where m_0 and m_t mean the mass of specimen before and after static oxidation experiments, respectively; t represents the oxidation time.

The phases of pyrolysis products from ZS and THC precursors, C/SiC-ZrC, and C/SiC-ZrC-HfC-TaC composites were analyzed by X-ray diffraction (XRD, Rigaku D/max2500) with Cu Kα radiation.

The microstructure and chemical composition of composites before and after the static oxidation tests were analyzed via field emission scanning electron microscope (SEM, SUPRA 55, ZEISS) equipped with energy dispersion spectroscope (EDS).

2 Results and Discussion

2.1 Static oxidation of C/SiC-ZrC composites

The appearances of C/SiC-ZrC composites before and after static oxidation at 1600 °C are shown in Fig. 2. Although C/SiC-ZrC composites suffer the severe tests, no cracks can be observed, indicating the good anti-oxidation and thermal

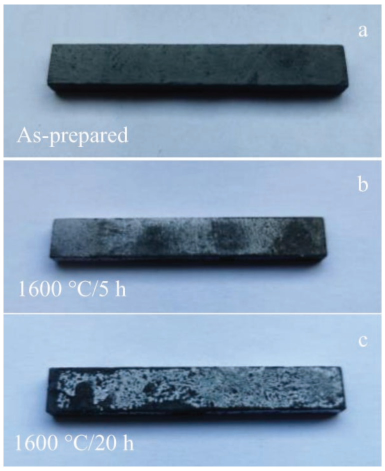

Fig.2 Appearances of C/SiC-ZrC composites before (a) and after static oxidation at 1600 °C for 5 h (b) and 20 h (c)

shock resistance of composites. As for the specimen after oxidation for 5 h, its surface is slightly oxidized and white oxides appear. With prolonging the oxidation duration to 20 h, the oxide layer becomes more evident on the specimen surface.

The calculation results of mass loss rate and flexural strength are summarized in Table 1. It can be seen that the flexural strength retention ratio of C/SiC-ZrC composites after oxidation for 5 and 20 h is 89.2% and 77.7%, respectively. The mass loss rates of C/SiC-ZrC specimens are 1.3×10^{-4} and 7.5×10^{-5} g/min after oxidation for 5 and 20 h, respectively. These results reveal that C/SiC-ZrC composites have good oxidation resistance.

The load-displacement curves of C/SiC-ZrC composites during three-point bending tests are shown in Fig. 3, and the pseudo-plastic fracture characteristics can be observed obviously. The curves present zigzag steps after reaching the maximum load, indicating the coupling effects of crack deflection, interfacial debonding, and fiber pulling-out. The load of C/SiC-ZrC specimens before and after oxidation reaches the maximum value and then decreases, resulting from serious oxidation reactions of composites. In addition, a linear relationship between the load and displacement can be observed for the three specimens at initial stage, which can be ascribed to the elastic deformation. Therefore, the cracks are easier to deflect along the interface of specimen after oxidation for 20 h according to its shortest linear segment.

2.2 Effects of HfC-TaC modification on oxidation resistance

In order to reveal the effects of HfC-TaC modification on high temperature oxidation performance of C/SiC-ZrC composite, the similar static oxidation tests were also conducted on the bending C/SiC-ZrC-HfC-TaC specimens. After oxidation at 1600 °C for 5 h, the specimen surface changes from black (Fig. 4a) to white (Fig. 4b), and a loose white oxidation layer forms. With prolonging the oxidation duration from 5 h to 20 h, the specimen still maintains the structural integrity (Fig. 4c), while the amount of oxide is not increased significantly.

Table 2 shows the mass loss rates and flexural strength of C/SiC-ZrC-HfC-TaC composites after static oxidation at 1600 °C. The flexural strength is decreased from 248 MPa to 227 and 181 MPa with prolonging the oxidation duration to 5 and 20 h, respectively. The high strength retention ratio (above 70%) suggests good oxidation resistance. As the oxidation duration increases from 5 h to 20 h, the mass loss rates are decreased from 7.3×10^{-5} g/min to 3.4×10^{-5} g/min.

It can be seen that the mass loss rate and flexural strength of both the C/SiC-ZrC and C/SiC-ZrC-HfC-TaC composites exhibit similar variation trends. The C/SiC-ZrC-HfC-TaC composite displays better behavior in terms of the mass loss, while the C/SiC-ZrC composite exhibits higher flexural strength.

The fracture behavior of C/SiC-ZrC-HfC-TaC composites after oxidation can also be characterized by the load-displacement curves (Fig. 5). Three curves all show an approximately constant slope in the initial stage and the peak

Table 1 Mass loss rates R_m and flexural strengths σ of C/SiC-ZrC composites before and after static oxidation at 1600 °C

Oxidation duration/h	Mass loss rate, R_m/g·min^{-1}	Flexural strength, σ/MPa	Strength retention ratio/%
As-prepared	-	332	-
5	1.3×10^{-4}	296	89.2
20	7.5×10^{-5}	258	77.7

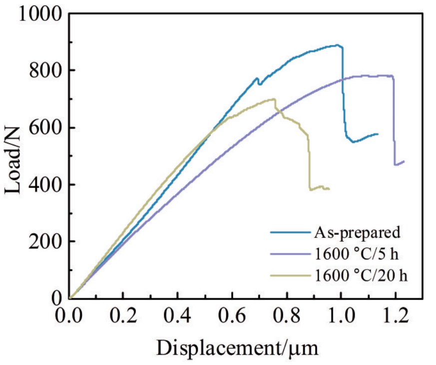

Fig.3 Flexural load-displacement curves of C/SiC-ZrC specimens before and after oxidation

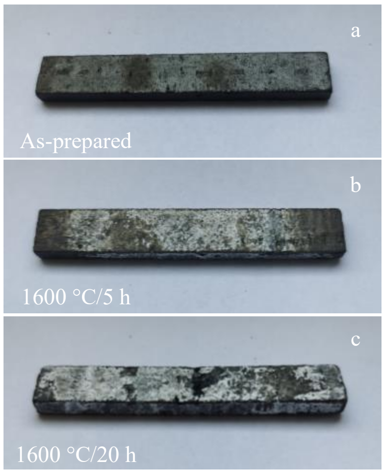

Fig.4 Appearances of C/SiC-ZrC-HfC-TaC composites before (a) and after static oxidation at 1600 °C for 5 h (b) and 20 h (c)

Table 2 Mass loss rates R_m and flexural strengths σ of C/SiC-ZrC-HfC-TaC composites before and after static oxidation at 1600 °C

Oxidation duration/h	Mass loss rate, R_m/$\times10^{-5}$ g·min^{-1}	Flexural strength, σ/MPa	Strength retention ratio/%
As-prepared	-	248	-
5	7.3	227	91.5
20	3.4	181	73.0

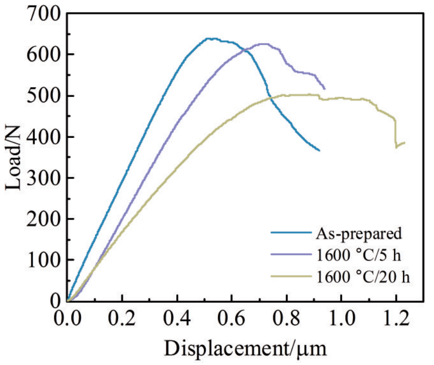

Fig.5 Flexural load-displacement curves of C/SiC-ZrC-HfC-TaC composites before and after static oxidation

appears in front of the long load retention zone. With the oxidation proceeding, the slope and the load value become smaller, indicating the decreased mechanical properties of composites. Considering the segment after the peak point, the loads of C/SiC-ZrC-HfC-TaC composites after static oxidation are decreased gradually through zigzag steps, and the composites do not show brittle fracture behavior. As for C/SiC-ZrC composites (Fig.3), their feature behavior is not as obvious as that of C/SiC-ZrC-HfC-TaC composites, especially under the oxidation condition of 1600 °C/5 h. Thus, the toughening effect is strengthened after HfC-TaC modification.

2.3 Oxidation behavior and mechanism

XRD patterns of pyrolysis products and composites are presented in Fig. 6. ZrC and SiC phases can be clearly observed in ZS pyrolysis products (Fig. 6a) and C/SiC-ZrC composites (Fig. 6c) with a small amount of residual carbon. This result suggests that ZS precursor is transformed into ZrC and SiC after pyrolysis process. Similarly, XRD analyses of THC pyrolysis product and C/SiC-ZrC-HfC-TaC composites are also shown in Fig. 6b and 6d, respectively. $Hf_xTa_yC_z$ phase is formed after pyrolysis, as indicated by the sharp diffraction peaks. ZrC and $Hf_xTa_yC_z$ phases play important parts in as-prepared C/SiC-ZrC-HfC-TaC composites.

Fig. 7 shows SEM cross-sectional morphologies of C/SiC-ZrC composites after different static oxidation tests. It can be seen that the SiC coating of as-prepared C/SiC-ZrC composites bonds well with the ceramic matrix (Fig. 7a), significantly protecting the composite from oxygen. After static oxidation at 1600 °C for 5 h, a large number of cavities appear in the coating region (Fig. 7d), which are caused by the release of byproducts, such as CO and SiO. Meanwhile, the cracks between coating and matrix become distinct (Fig. 7b), demonstrating that the SiC-ZrC matrix is responsible for the overall oxidation resistance of composites. As the oxidation time is extended from 5 h to 20 h, the significant mass loss of matrix around carbon fibers can be observed in Fig. 7c. This phenomenon suggests that SiC-ZrC matrix cannot provide efficient protection for inner carbon fibers after continuous oxidation at 1600 °C for 20 h.

The cross-sectional morphologies of HfC-TaC-modified C/SiC-ZrC composites are shown in Fig. 8. The microstructure of as-prepared C/SiC-ZrC-HfC-TaC composites exhibits the similar features to that of C/SiC-ZrC composites. The introduction of HfC-TaC does not lead to the detachment in the composite matrix (Fig. 8a), presenting a strong bonding interaction between SiC, ZrC, HfC, and TaC, which is beneficial to the improvement of oxidation resistance. After

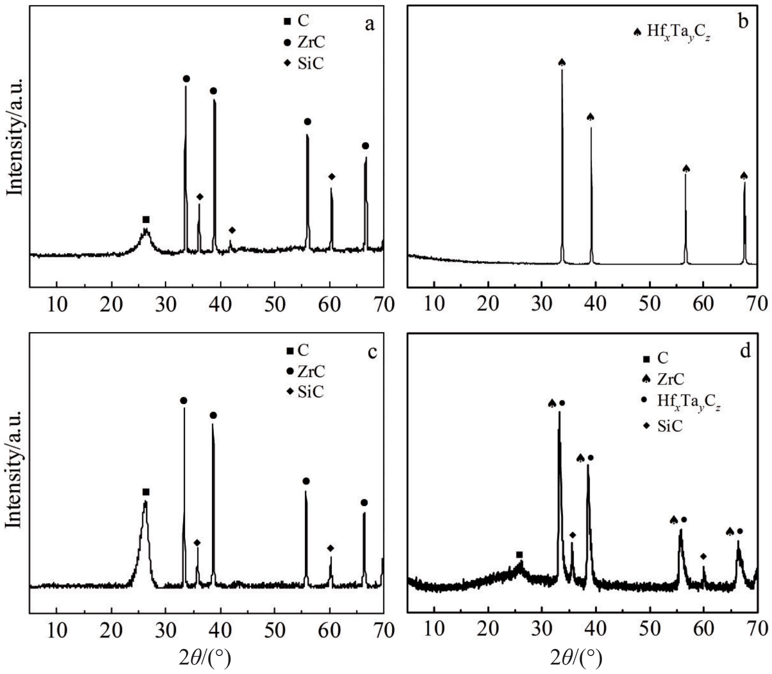

Fig.6 XRD patterns of pyrolysis products of ZS (a), THC precursors (b), C/SiC-ZrC composites (c), and C/SiC-ZrC-HfC-TaC composites (d)

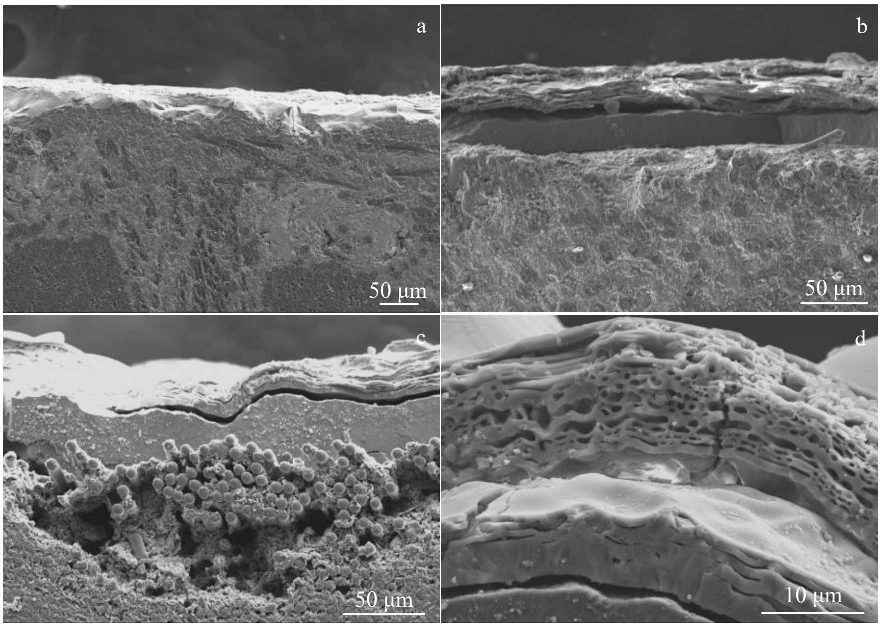

Fig.7 SEM cross-sectional morphologies of C/SiC-ZrC composites before (a) and after oxidation at 1600 °C for 5 h (b) and 20 h (c, d)

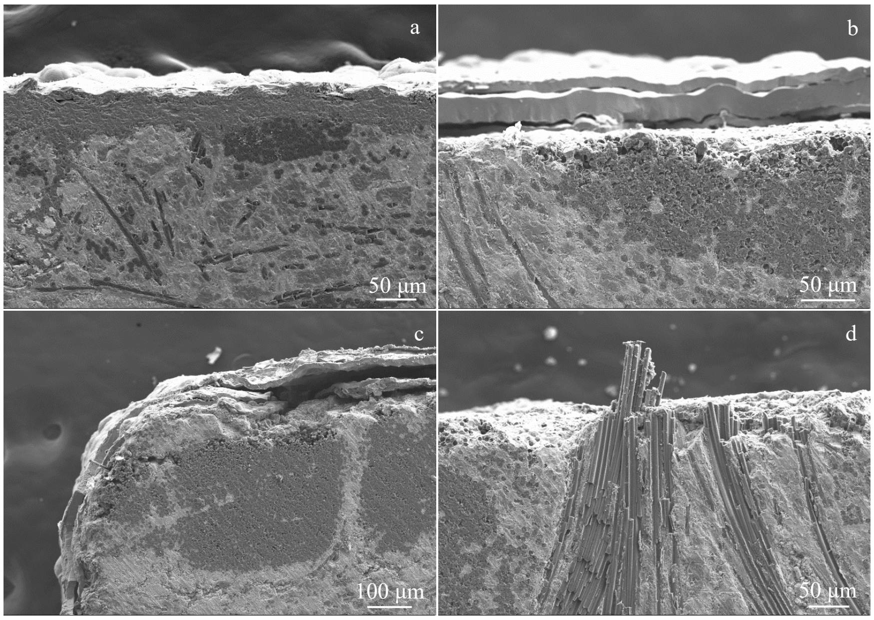

Fig.8 Cross-sectional morphologies of C/SiC-ZrC-HfC-TaC composites before (a) and after oxidation at 1600 °C for 5 h (b) and 20 h (c, d)

oxidation at 1600 °C for 5 h, the C/SiC-ZrC-HfC-TaC composites are similar to C/SiC-ZrC composites (Fig. 8b). However, after oxidation at 1600 °C for 20 h, SiC-ZrC-HfC-TaC matrix is still compact (Fig. 8c). In the specific regions where SiC coating is consumed (Fig. 8d), the matrix with carbon fibers remains nearly intact. Hence, the addition of HfC-TaC can offer superior protection for carbon fibers.

The even element distribution is important to achieve the high oxidation resistance at high temperature. SEM morphology and corresponding EDS element distributions of C/SiC-ZrC-HfC-TaC composites after oxidation at 1600 °C for 20 h are shown in Fig.9. It can be clearly observed that the Si, Zr, Hf, Ta, and O elements are distributed evenly after the oxidation, and they exist in the form of corresponding oxides in the composite. In addition, the ceramic matrix with carbon fibers remains compact without cracks. Therefore, the superior anti-oxidation properties of C/SiC-ZrC-HfC-TaC composites result from the dense structure and uniform elemental distribution.

3 Conclusions

1) C/SiC-ZrC and C/SiC-ZrC-HfC-TaC composites can be fabricated via combined process of precursor infiltration and

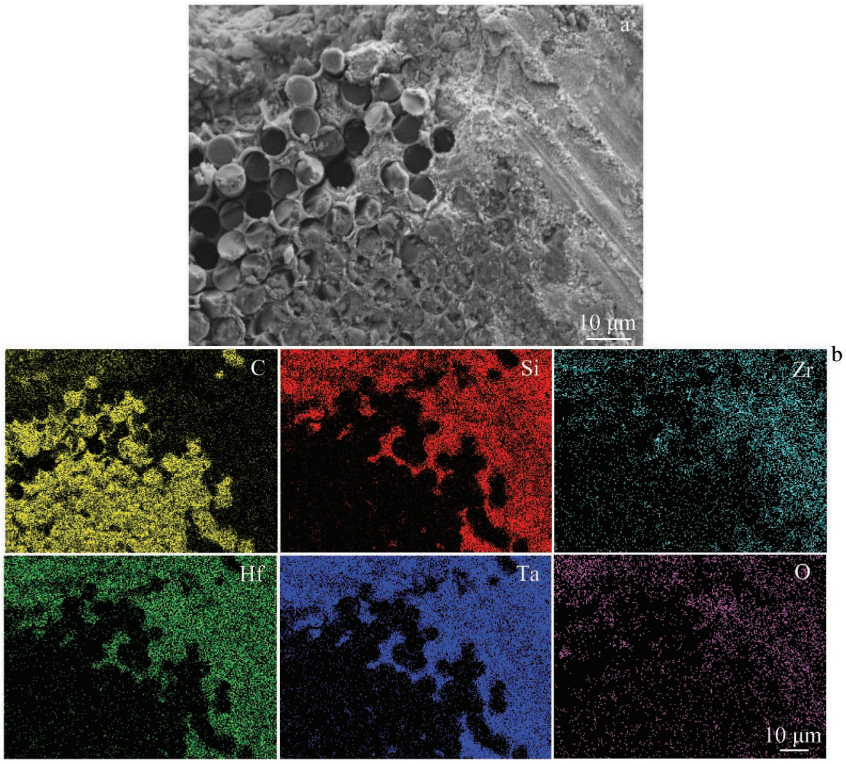

Fig.9 SEM cross-sectional morphology (a) and corresponding EDS element distributions (b) of C/SiC-ZrC-HfC-TaC composites after static oxidation at 1600 °C for 20 h

pyrolysis (PIP) method and chemical vapor deposition (CVD) method.

2) HfC-TaC modification can effectively improve the oxidation resistance of C/SiC-ZrC composites, and the mechanical properties of composites are still reasonable.

3) The well-integrated matrix and uniform element distribution are responsible for the enhanced anti-oxidation properties of C/SiC-ZrC-HfC-TaC composites.

References

1 Konrinoa S A, Gee K, Prabhu D K. *35th AIAA Thermophysics Conference*[C]. Anaheim: American Institute of Aeronautics & Astronautics, 2001: 2886

2 Paul A, Venugopal S, Binner J G P *et al. Journal of the European Ceramic Society*[J], 2013, 33(2): 423

3 Tang S F, Hu C L. *Journal of Materials Science & Technology* [J], 2017, 33(2): 117

4 Jin X C, Fan X L, Lu C S *et al. Journal of the European Ceramic Society*[J], 2018, 38(1): 1

5 Rubio V, Ramanujam P, Binner J. *Advances in Applied Ceramics* [J], 2018, 117(S1): 56

6 Fahrenholtz W G, Wuchina E J, Lee W E *et al. Ultra-High Temperature Ceramics: Materials for Extreme Environment Applications*[M], New York: Wiley, 2014

7 Sciti D, Silvestroni L, Monteverde F *et al. Advances in Applied Ceramics*[J], 2018, 117(S1): 70

8 Sciti D, Zoli L, Silvestroni L *et al. Materials and Design*[J], 2016, 109: 709

9 Dai Jixiang, Sha Jianjun, Wang Yongchang *et al. Rare Metal Materials and Engineering*[J], 2016, 45(3): 742 (in Chinese)

10 Zhou H J, Ni D W, He P *et al. Ceramics International*[J], 2018, 44(5): 4777

11 Chen S A, Zhang C R, Zhang Y D *et al. Corrosion Science*[J], 2013, 68: 168

12 Li Q G, Dong S M, Wang Z *et al. Journal of Asian Ceramic Societies*[J], 2015, 3(4): 377

13 Zhou C L, Liu D Z, Zhi W *et al. Materials Research Innovations* [J], 2015, 19(S1): 375

14 Wang Yanbin, Su Xunjia, Hou Genliang *et al. Rare Metal Materials and Engineering*[J], 2008, 37(4): 729 (in Chinese)

15 Cheng Jun, Zhang Jizhou, Wang Xiaozhou *et al. Rare Metal Materials and Engineering*[J], 2018, 47(S2): 108

16 Cedillos-Barraza O, Manara D, Boboridis K *et al. Scientific Reports*[J], 2016, 6: 37 962

17 Shimada S, Yunazar F, Otani S. *Journal of the American Ceramic Society*[J], 2000, 83(4): 721

18 Chen Z K, Xiong X. *Materials Chemistry and Physics*[J], 2013, 141(2-3): 61

HfC-TaC改性对C/SiC-ZrC复合材料静态氧化行为的影响

陈昊然，杨良伟，张宝鹏，刘　伟，宋环君

(航天特种材料及工艺技术研究所，北京 100074)

摘　要：利用HfC-TaC对C/SiC-ZrC陶瓷基热结构复合材料进行改性，提升C/SiC-ZrC材料的抗氧化性能。结合前驱体浸渍裂解和化学气相沉积法制备陶瓷基复合材料，并通过静态氧化实验（1600 ℃/5 h和1600 ℃/20 h）检验其抗氧化性能。结合弯曲强度测试和失重情况分析，发现HfC-TaC可以有效改善C/SiC-ZrC复合材料的氧化行为，且能够使其满足力学性能要求。借助X射线衍射仪、扫描电子显微镜和能谱仪等仪器，对复合材料的晶相结构、微观结构等进行了分析，结果显示：均匀的元素分布和基体中各陶瓷组元间良好的融合度是C/SiC-ZrC复合材料抗氧化性能提升的原因。

关键词：HfC-TaC；C/SiC-ZrC；陶瓷基复合材料；静态氧化；前驱体浸渍裂解

作者简介：陈昊然，男，1993年生，博士，工程师，航天特种材料及工艺技术研究所，北京 100074，E-mail：chenhaoran@pku.edu.cn